Research article

Geochemical characteristics and implications of hydrocarbon in source rocks of Chagan Sag, Yin'e basin of Inner Mongolia

Wenjie Xiao [a,b], Hong Ji [a,*], Guanghui Huang [b,**]

[a] College of Science, Guangdong University of Petrochemical Technology, Maoming Guangdong 525000, China
[b] College of Resources and Environment, Yangtze University, Wuhan 430100, Hubei, China

ARTICLE INFO

ABSTRACT

Chagan Sag is one of the most significant tectonic unit in the Yin'e Basin. The special component of the organic macerals and biomarkers in the Chagan sag suggests great difference of its hydrocarbon generation process. In this paper, forty samples of source rocks are subjected to carry out on the geochemical characteristics by methods of rock-eval analysis, organic petrology and gas chromatography mass spectrometry (GC-MS) to reveal the origin, depositional environment and maturity of organic matter in Chagan Sag, Yin'e Basin of Inner Mongolia. The total organic matter of the analyzed samples ranges from 0.4 wt%~3.89 wt% with an average of 1.12 wt%, indicating fair to excellent hydrocarbon generation potential. The rock-eval results show that the S_1+S_2 and hydrocarbon index range from 0.03 mg/g~16.34 mg/g (avg.3.6 mg/g) and 6.24–521.32 mg/g (avg. 199.63 mg/g), suggesting most of the kerogen types are type II and III, with small amount of type I. The Tmax ranges from 428 to 496 °C, suggesting low mature to mature stage. The macerals component of morphological macerals presents with certain amount of vitrinite, liptinite and some inertinite. However, the amorphous component takes the dominant part of the macerals with account of 50%–80%. The amorphous components are dominated by sapropelite in the source rock, indicating bacteriolytic amorphous promote the organic generation process. Hopanes and sterane are widely distributed in the source rocks. The biomarker results suggest a mix of planktonic-bacterial and higher plant origins, with wide range of thermal maturity and relatively reducing depositional environment. Abnormal high content of hopanes were observed in the biomarkers, and some special biomarkers such as monomethylalkanes, long-chain-alkyl naphthalenes, aromatized de A-triterpenes, 8,14-seco-triterpenes, and A, B-cyclostane are detected in Chagan Sag. The presence of these compounds suggests that bacterial and microorganisms are of great significance to the generation of hydrocarbon in the source rock in Chagan Sag.

1. Introduction

Microorganisms are important material basis for the formation of organic matter in source rocks [1,2]. The development of microorganisms in the sedimentary diagenetic stage can provide organic matter for the sediments and improve the primary biological productivity [3]. The large number of microorganisms can also create an anoxic depositional environment and form a relatively

* Corresponding author.
** Corresponding author.
E-mail addresses: jihong@gdupt.edu.cn (H. Ji), GH-Huang-389241528@qq.com (G. Huang).

reducing environment, which is conducive to the preservation of organic matter [4,5]. The anaerobic microorganisms degrade the original sedimentary organic matter, which is continuously transformed by microorganisms and can be converted into substances that are more likely to generate hydrocarbons, such as bacteria-degraded amorphous bodies and sapropelic kerogen after sedimentation and burial [6]. Therefore, the development of microorganisms in the sedimentary diagenetic stage and their transformation of organic matter are of great significance to the generation of organic matter in source rocks. The sedimentary organic matter of the source rock is mainly composed of two parts, one is the organic maceral with morphology, and the other is the organic matrix component without morphology and mineral bitumen matrix [7,8]. Organic maceral identification is the most intuitive method to recognize the types of hydrocarbon-forming original parent materials and organic matter in source rocks.

Chagan Sag, located in the eastern Yingen-Ejinaqi Basin ("Yin'e Basin" for short), has one of the largest sedimentary Mesozoic thicknesses with a total resource amount of 139 million tons in an exploration area of about 2000 km^2, indicating great hydrocarbon potential for this area [9,10]. The maceral components and biomarkers from extract of source rocks of Chagan Sag shows the origin of the crude oil in Chagan Sag is quite special. Hydrocarbon accumulation patterns and geologic features of Chagan Sag were reported [11–14]. At present, the specific causes of the origin of crude oil in the Chagan Sag are unclear. In this paper, the composition of kerogen macerals and characteristics of biomarkers of the source rocks are analyzed. Then depositional environment and origin of the organic matter are deciphered and the influence and contribution of microbial action on hydrocarbon-generating organic matter are discussed in the end. The objectives of this study are use the biomarkers and organic petrology approaches to illustrate the hydrocarbon generation characteristics of source rocks in Chagan Sag, Yin'e basin of China.

1.1. Geological setting

The Chagan Sag is in the Yingen-e'jinaqi Basin in Inner Mongolia ("Yin'e Basin" for short) (Fig. 1a) presented with a pan-like shape (Fig. 1b). The basement of the depression is more than 6000 m deep. The upper and lower Cretaceous and Cenozoic strata are the main sedimentary strata in the Chagan Sag with the Triassic and Jurassic missing. The main part of the Chagan Sag is an inland-faulted basin
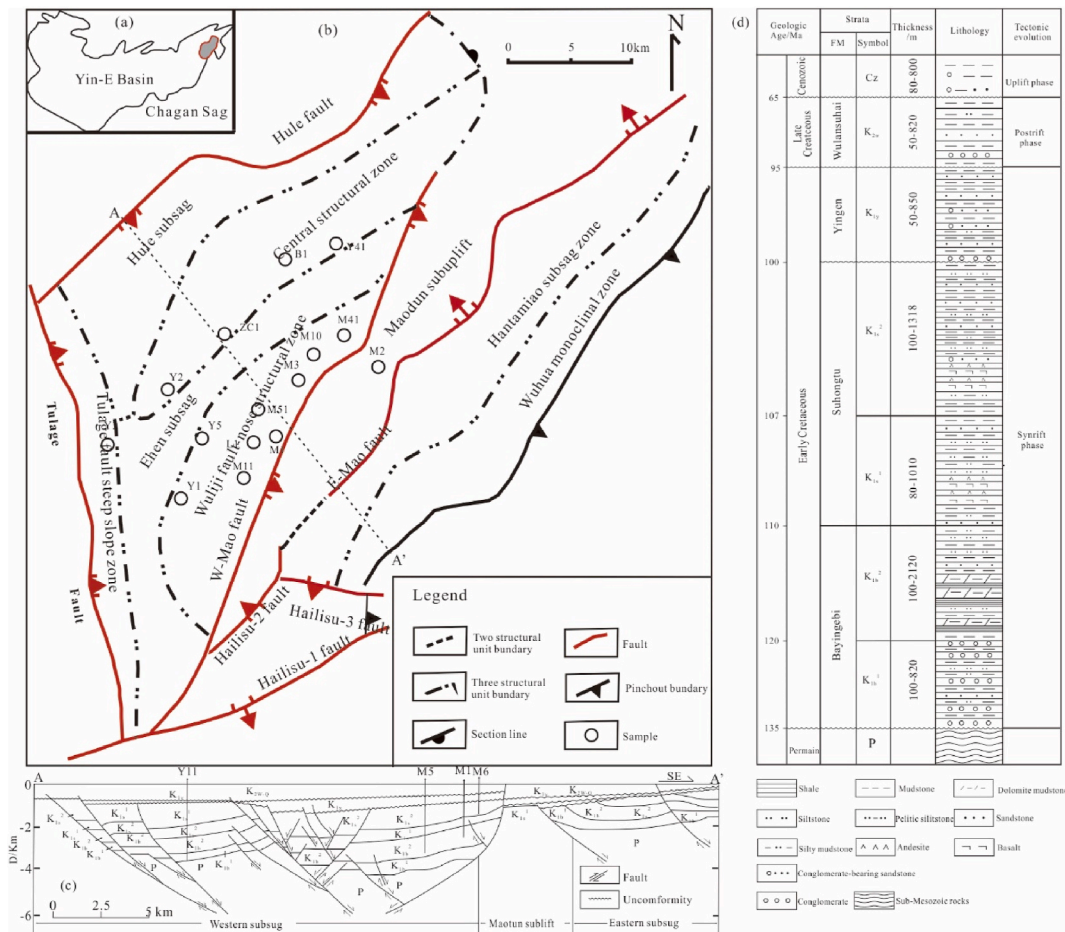

Fig. 1. (a) Chagan Sag in Yin-e Basin; (b) Structural unit division of the Chagan Sag; (c) Structural profile map; (d) Stratigraphic column map of Chagan Sag.

developed on the fold basement of the Late Paleozoic (Fig. 1c). Affected by the Hercynian movement, only two strata developed in the sag: Cretaceous and Cenozoic. The sedimentary strata from bottom to top are the Lower Cretaceous Bayingebi Formation (K_1b_1 and K_1b_2), the Suhongtu Formation (K_1s), the Yingen Formation (K_1y), the Upper Cretaceous Wulansuhai Formation (K_2w), and the Cenozoic Paleogene (Cz) (Fig. 1d). Among them, the K_1b_2 can be further divided into $K_1b_2^U$ and $K_1b_2^L$. It is a typical half graben-like rift lake basin developed on the late Paleozoic folded basement and faulted in the southwest and northeast. The stratum is thick in the west and thin in the east. Faults are well developed in the sag, mainly extending in the north-east direction, and divided the sag into western sub-sags (Hule subsag belt, central structural belt, Ezo subsag belt, Wuliji structural belt), Maodun sub-convex, and eastern sub-sag (Hantamiao subsag belt, Wuhua monoclinic belt, Hailisu thrust belt), showing a pattern of alternating concavities and convexities (Fig. 1b). During the depositional period of the Bayinggobi Formation (K_1b), the depression was mainly composed of a set of nearshore subaqueous fan facies, fan delta facies, braided river delta facies and lacustrine facies, and the lithology was mainly gray glutenite, sandstone, argillaceous siltstone, dark gray and mudstones with different thicknesses (Fig. 1d). The Suhongtu Formation develops multiple sets of volcanic rock-shallow lake interbedded sediments. The upper lithology of Suhongtu Formation (K_1s) are mainly brownish gray, dark gray mudstone and siltstone, sandstone, gravel sandstone and black basalt interbedded (Fig. 1d). The lithology of lower Suhongtu Formation (K_1s) is mainly gray, dark gray mudstone, silty mudstone mixed with siltstone, sandstone mixed with black basalt and gray-green andesite (Fig. 1d). During the depositional period of the Yingen Formation (K_1y), it is a set of braided fluvial facies, with red and brown mudstone and silty sandstone, and mudstone intercalated with sandstone and conglomerate deposits (Fig. 1d).

2. Materials and methods

In this study, source rock samples from three different stratums were collected in the Chagan Sag, which were from the first member and second member of Bayinggebi Formation (K_1b_1 and K_1b_2) and first member of Suhongtu Formation (K_1s_1). Source rock samples are subjected to microscopic identification of macerals, extraction of soluble organic matter, separation of group component and GC/MS analysis of saturated hydrocarbons and aromatics.

202 samples were used to quantify the organic maceral. Samples were crushed and sieved to a range size of 60–80 mesh, cemented with epoxy resin, and prepared into a particle light sheet. According to the characteristics and the color, shape, and intensity of fluorescence under the Leica DM4500P polarizing microscope, the organic macerals were identified and the contents were analyzed by statistical methods. Chinese standard SY/T 6414 was adopted to classify maceral [15].

The total organic carbon (TOC) content (wt.%), rock-eval pyrolysis and Gas chromatography-mass Spectrometer (GC-MS) analysis were conducted on forty source rocks. The total organic carbon content was determined by LECO CS-200 elemental analyzer with a precision of 0.5 wt%. About 10 mg of each powered sample was analyzed after digesting with dilute HCl (HCl/H_2O, 1:7) at 70 °C for 2 h to remove carbonates and dried. Rock-eval pyrolysis was carried out by a rock-eval II instrument. Samples with powdered was heated at a rate of 300°C–500 °C in a He atmosphere to obtain S_1, S_2, S_3 and T_{max}. The parameters S_1, S_2, S_3 and T_{max} represent free hydrocarbon, thermal cracked hydrocarbon, carbon dioxide generated from organic matter and maximum temperature from S_2, respectively.

Soxhlet extraction method was applied to extractable organic matter for 72 h with an azeotropic mixture of chloroform/methanol (87:13). The extracted organic matter was separated into saturated fractions, aromatic fractions and polar by the column chromatography method.

The saturated fractions were carried out on 6890 N/5975I chromatographic mass spectrometer. The chromatographic column is HP~5MS quartz elastic capillary column (30 m × 0.25 mm × 0.25 μm). The temperature-raising program is a constant temperature of 50 °C for 1 min, then a temperature of 20 °C/min from 50 °C to 100 °C, and then a temperature of 3 °C/min from 100 °C to 315 °C, and a constant temperature of 315 °C for 20 min. The temperature of the sampler is 300 °C. The carrier gas is helium, and the flow rate is 1.0 mL/min. The scanning range is 50~550amu.

The aromatic fractions were carried out on a 6890 N/5973 chromatographic mass spectrometer. The chromatographic column is HP-5MS quartz elastic capillary column (60 m × 0.25mm × 0.25 μm). The heating procedure is constant temperature at 50 °C for 1 min, then from 50 °C to 150 °C at 8 °C/min, then from 150 °C to 310 °C at 4 °C/min, and finally constant temperature at 310 °C for 23min. The temperature of injector is 290 °C, and the carrier gas is helium, and the flow rate is 1.0 mL/min. Multi-ion detection and full scan were adopted. The mass spectrometry conditions are: +EI/QIMS, and the ionization energy of the ion source is 70eV. The mass scanning range is 50–550amu, and the scanning interval is 2s.

3. Results

3.1. Hydrocarbon generation potential

Hydrocarbon generation potential is the ability of a rock to generate hydrocarbons, such as oil and gas, from organic matter. This potential is determined by the types of rock, the amount of organic matter abundance, and the thermal maturity. The higher the hydrocarbon generation potential, the more likely it is that hydrocarbons will be generated. In this study, organic matter abundance and types were evaluated by total organic carbon (TOC) and rock-eval analysis. The results show that source rocks are mudstone and organic matter abundance with TOC ranging from 0.4–3.87 wt% (avg.1.12 wt%) and S_1+S_2 values ranging from 0.03–16.34 mg HC/g rock (avg. 3.6 mg HC/g rock). According to the evaluation criteria proposed by Peters and Cassa (1994) [16], most of the samples are classified as fair to good source rocks (Fig. 2). Among the three formations, samples from K_1b_1 and K_1b_2 bear better hydrocarbon

generation potential and the K_1s_1 shows less organic matter abundance and generation production (Fig. 2).

The type of organic matter is also important parameters in source rock evaluation. Generally, type I kerogen is oil-prone of sapropel type and type III is gas-prone of humic type. The organic matter types are determined by hydrocarbon index (HI) and maceral composition. The hydrocarbon index (HI) of the analyzed samples ranges from 6 to 521 mg HC/g TOC (with the average value of 199.6 mg HC/g TOC) and the T_{max} ranges from 428 °C to 496 °C, indicating low mature to mature stage (Fig. 3). The kerogen type of the analyzed samples is primarily classified as type II and III. Some samples from K_1b_2 shows type I features. The kerogen types of Chagan Sag reveal complicated origins of the organic matter for hydrocarbon.

3.2. Composition of kerogen macerals

The organic matter in source rock is created by the formation and deposition of biological organic matter after biochemical action [17–19]. The maceral is solid organic matter formed by diagenesis of organic matter from different sources [20]. Kerogen is composed of a variety of macerals, including liptinite, inertinite, and vitrinite. Liptinite macerals are derived from plant material and are composed of alginite, cutinite, and resinite. Inertinite macerals are derived from the remains of woody material and are composed of fusinite, semifusinite, and inertodetrinite. Vitrinite macerals are derived from the remains of plant material and are composed of collotelinite, telinite, and vitrodetrinite. Vitrinite, inertinite and liptinite were detected in the fluorescence analyses of studies samples (Fig. 4). Among them, vitrinite including telinite (Fig. 4a, e) and detrogelinite (Fig. 4d), inertinite such as inertodetrinite (Fig. 4b, e) and fusinite (Fig. 4c), liptinite including sporinite and lamalgnite (Fig. 4e and f) are shown in Fig. 4. Framboidal pyrite also observed (Fig. 4b), suggesting reducing environment for the organic matter accumulation.

The kerogen of source rock in different formations in Chagan Sag is mainly composed of amorphous components with content of 53.79%–69.46%. and the morphological components only counts for 50.54%–46.2% (Fig. 5, Table 1). Of the morphological components, vitrinite content takes the dominant part with amount of 20.83%–32.28%, followed by exinite, accounting for 2.53%–9.61%, inertinite (1.79%–5.96%) and alginate (0.17%–2.35%), respectively (Figs. 4 and 5, Table 1). The exinite is mainly composed of sporophyte and cutinite while resinite is underdeveloped. The content of amorphous organic matter, which are principally identified as humic amorphous is high with ranges of 53.79%–69.64% (Fig. 5, Table 1). The amorphous components of source rocks in the Chagan Sag are dominated by sapropelite and huminte organic matter with amount of 16.5%–35.48% and 22.27%–37.80%, respectively (Table 2). It also contains a certain amount of mycetoma, cutinite and resinite (Figs. 4 and 5 and Table 2). Amorphous organic matter is mostly related to the action of microorganisms (bacteria), except for parts that may be derived from the waxy part of higher plants [21, 22]. The sapropelite content in K_1s_1 and K_1b_2 are quite high indicating that bacteriolytic amorphous make significant contribution to organic matter formation.

3.3. Characteristics of biomarkers

The n-alkanes in the source rock of Chagan Sag are primarily unimodal (Fig. 6). The content of low molecular weight compounds is much less but compounds with medium to high molecular weight are higher with nC_{23} as the main peak in some source rocks (Fig. 6). Source rocks with relatively shallow burial depths and high-number of carbon n-alkanes show an odd-even predominance (Fig. 6), which probably indicates the contribution of higher plant biogenic sources [23]. One thing worth noting is that abnormal high amount of hopanes were observed in the saturated hydrocarbon fractions in Fig. 6f, indicating that bacterial organic matter has significant contribution to hydrocarbon generation.

Sterane and terpanes are abundant in the soluble organic matter of source rock in Chagan Sag (Fig. 7). The terpenoids are dominated by pentacyclic triterpanes, and hopanes are abundant and even exceed the relative abundance of n-alkanes in the total oil ion chromatography (TIC) (Fig. 6). Pentacyclic triterpene of Chagan Sag shows relatively wide range of tricyclic terpane abundance
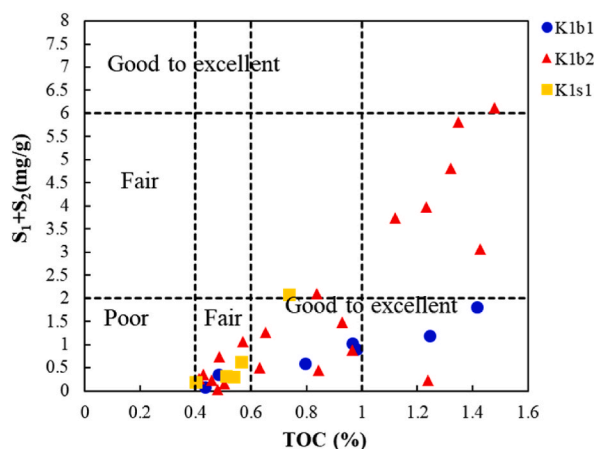

Fig. 2. Variation of rock-eval S_1+S_2 with total organic carbon (TOC), showing the hydrocarbon generation potential.
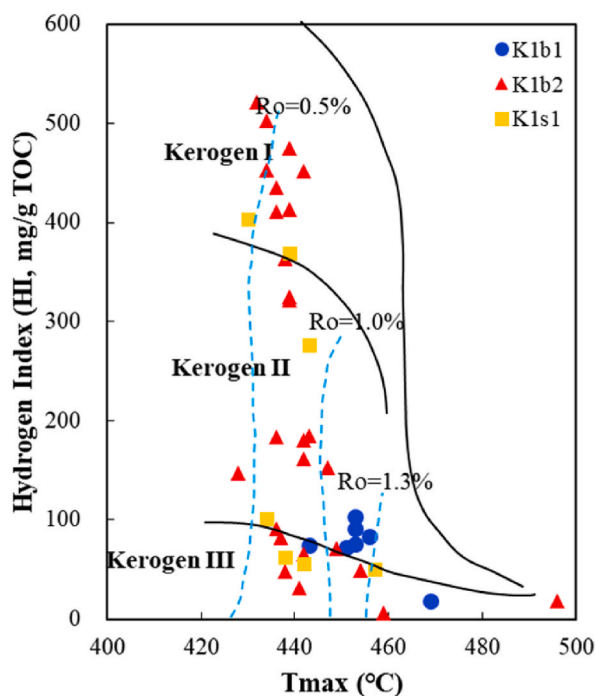
Fig. 3. Variation of rock-eval hydrogen index (HI) with Tmax for analyzed samples, showing thermal maturity and hydrocarbon generation potential.
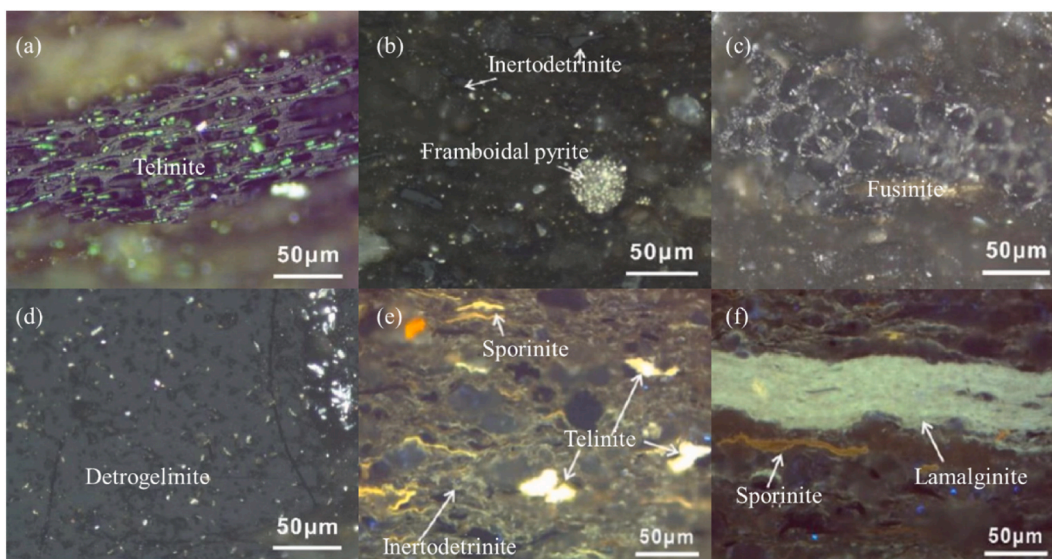

Fig. 4. Microscopic images showing the maceral components of in kerogen of Chagan Sag, Yin'e basin. (a) Telinite, (b) Inertodetrinite and framboidal pyrite, (c) Fusinite, (d) Detrogelinite, (e) Sporinite, telinite and inertodetrinite, (f) Sporinite and lamalgnite.

and rich in homohopanes and gammacerane with C_{30} hopane as the main compound (Fig. 7 left). High content of gammacerane were observed, which indicates a density-stratified water column, commonly resulting from hypersalinity at depth [24,25]. The abundant of gammacerane in Chagan Sag suggest it was a closed water sedimentary environment during organic matter deposition. The steranes are mainly regular C_{27}~C_{29} steranes with wide range of low molecular weight pregnanes and diasteranes (Fig. 7 right). Previous study noted that higher concentrations of C_{29} steranes in carboniferous and younger sediments are generally attributed to terrestrial plants while higher concentration of C_{28} and C_{27} steranes suggest input of organic matter(phytoplankton) from lacustrine and marine environments, respectively [23,24]. Among the regular steranes, the distribution of C_{27}~C_{29} steranes of Chagan Sag shows a V-shaped
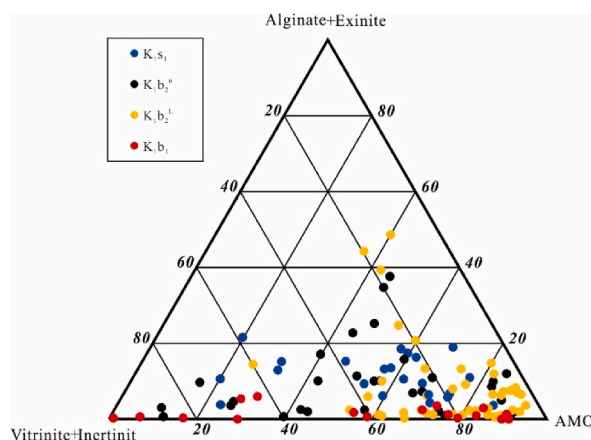
Fig. 5. Ternary diagram showing the maceral composition of kerogen in source rock of Chagan Sag are primarily amorphous components.

Table 1
Content of macerals in kerogan from Chagan Sag.

Fm.	Sample No.	Morphological maceral content of kerogen , %					Amorphous components
		Vitrinite	Inertinite	Exinite	Alginate	Morphological components	
K_1s_1	58	30.66	3.02	7.32	1.26	42.26	57.74
$K_1b_2^U$	51	32.39	3.19	9.61	1.02	46.2	53.79
$K_1b_2^L$	64	20.83	1.79	5.57	2.35	30.54	69.46
K_1b_1	29	32.28	5.96	2.53	0.17	40.94	59.06

Table 2
Content characteristics of amorphous components of source rock in Chagan Sag.

Fm.	Sample No.	Sapropelite (%)	Huminite (%)	Mycetome (%)	Sporinite (%)	Cutinite (%)	Resinite (%)
K_1s_1	58	35.48	22.27	0.11	3.05	4.09	0.04
K_1b_2	115	30.10	31.53	0.12	3.51	3.63	0.02
K_1b_1	29	16.50	37.80	0.18	1.02	1.24	0

and some samples are taking C_{29} steranes as the dominant one and some samples are occupied by C_{27} (Fig. 7 right), reflecting the contribution of higher plants and mixed origins from their parent material sources. The various content of diasteranes also suggest that samples vary widely in maturity (Fig. 7 right).

4. Discussion

4.1. The origin of the organic matter

Hopanes are quite abundant in several samples, which even exceeding the abundance of n-alkanes for some samples (Figs. 6 and 7 left). The ratio of hopane/sterane for K_1s_1, K_1b_1 and K_1b_2 are 0.17–2.21 (1.12), 0.87–1.64 (1.34) and 0.22–4.53 (1.36), respectively (Table 3). The precursors of hopanoids are "biohopanoids", whose compounds are generally derived from some special bacteria [26, 27]. The abnormally high content of hopane suggest that bacterial biogenic organic matter contribute significant in hydrocarbon generation. Regular steranes are good indicators to decipher the organic matter input. The m/z 217 mass fragments of the samples are characterized by high amount of C_{29} and C_{27} regular steranes relative to C_{28} regular sterane (Fig. 7 right), with the relative proportion of C_{27}, C_{28} and C_{29} regular steranes in the range of 16.94%–50.87%, 12.78%–33.29%, and 32.97%–58.87%, respectively (Table 3). These distributions of C_{27}–C_{29} regular steranes also reflect a mixed of planktonic-bacterial organic matter and land plant input as demonstrated by the ternary diagram of regular steranes (Fig. 8).

Dissolved organic matter in source rock is the product of hydrocarbon-generating organic matter [28,29]. Isoalkanes represent a major (10–25%) petroleum component [30]. The results show that the composition of soluble organic matter in source rock in Chagan Sag has obvious particularity. A complete series of monomethyl paraffin compounds were observed in the source rock of different formations in Chagan Sag (Fig. 9), and isomers of monomethyl alkanes compounds with different carbon numbers were also detected in source rocks, which mainly indicate the contribution of bacterial waxy biogenic sources [31–33]. Generally, isoalkane (2-methyl-) and anteisoalkane (3-methyl-) have stronger M − 43 and M − 29 fragments; 4-methyl- alkanes have stronger M − 43 fragments, and
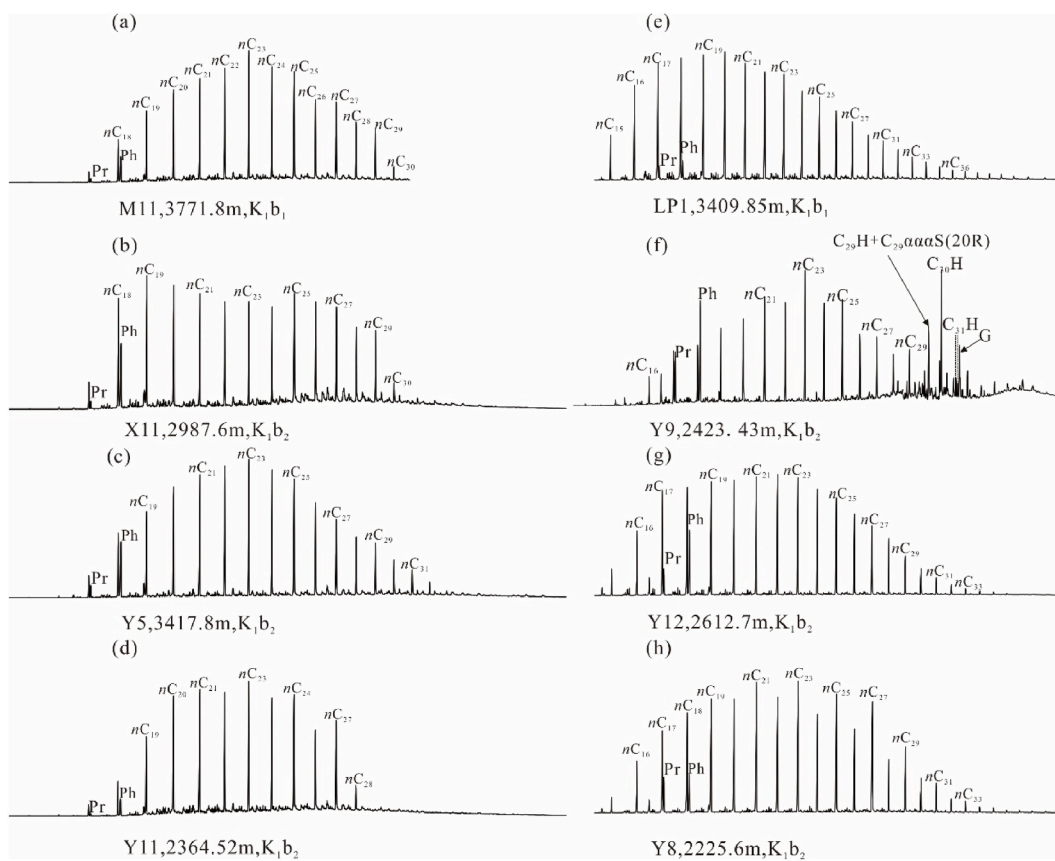
Fig. 6. Distribution characteristics of n-alkanes in source rock of Chagan Sag.

5-methyl have stronger M − 57 fragments, respectively (Fig. 9). The closer the methyl group is to the middle of the alkane carbon chain, the higher the peak. In addition, several compounds with methyl groups near the middle of common chromatographic columns often escape and form the "X" compound (Fig. 9). The detection of these compounds and the abundant hopanes in the saturated hydrocarbon fractions of the source rock in the Chagan Sag indicate that bacterial biogenic organic matter makes an important contribution to hydrocarbon generation.

A pair of series straight long-chain alkyl naphthalenes (aNs) with alkyl chain carbon number up to 31 was detected (Fig. 10). Abundance of long-chain alkyl naphthalenes in source rocks and crude oils are usually suggesting *Botryococcus braunii* or *Gloeocapsomorpha Prisca* input [34], implying an algal source relationship [24]. The distribution of these compounds is positively correlated with the relative abundance of bacterial biogenic rock compounds, and it is speculated that the genesis of these compounds is related to the biogenic contribution of microorganisms. The detection of this compound in the Chagan Sag also suggests the biogenic contribution of microorganisms in the original organic matter of the source rock.

Tricyclic terpenoids are mainly formed by tricyclic isodienols in microbial cell membranes, and may also be related to the formation of some algae [24]. They are compounds of lower biogenic origin of bacteria and algae, and are commonly observed in marine or lake sediments. When higher plants have undergone strong microbial transformation, orlanane, ursane and lupine often remove the A-ring to form de-A-tricyclic terpenes, and form 8,14-seco-hopanes compounds at the same time [35,36]. Compounds of A-triterpenes such as des-A-lupane and des-A-ursanne, respectively were observed in Chagan Sag (Figs. 11 and 12). A-triterpenes with different aromatization degrees (Fig. 11) and aromatized 8,14-seco-hopanes (Fig. 12) are symbolic compounds of the bacterial transformation of higher plants. The occurrence of these compounds in source rock indicates that the metabolic process of bacteria is of great significance in the formation of hydrocarbon-generating organic matter in the source rock of Chagan Sag by regenerating the organic matter.

In addition, abundant des-A, B-cyclostane have been detected in the source rock of different stratum in Chagan Sag (Fig. 13), and the distribution of such compounds is rare. According to the analysis of genetic characteristics of related compounds in Figs. 11 and 12, the formation process of des-A, B-cyclostane maybe be related to the action of microorganisms.

4.2. Hydrocarbon generation with microbial process

Positive correlation between the TOC and the hydrogen index (HI) of lacustrine facies are observed (Fig. 14). With the decrease of TOC, HI decreases (Fig. 14). Bacterial organic matter is regenerated organic matter formed by the anabolism of chemotropic
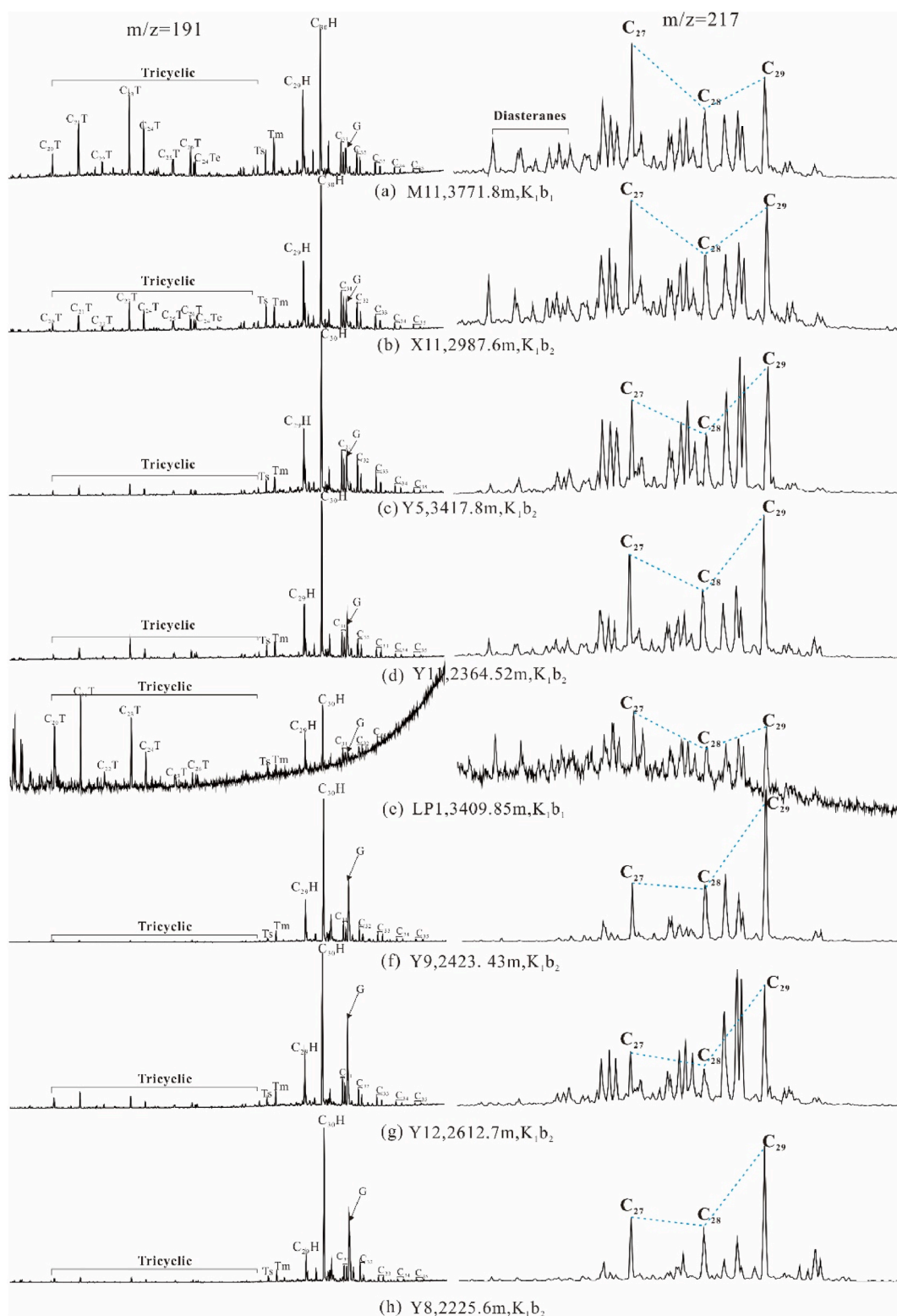
Fig. 7. Mass chromatograms of pentacyclic triterpene *m/z* 191 (left) and sterane *m/z* 217 (right) of source rock in Chagan Sag.

Table 3
Geochemical parameters of source rocks in different strata in Chagan Sag.

Well ID	Depth (m)	Fm.	TOC (%)	Tmax (°C)	S_1+S_2 (mg/g)	HI (mg/g)	Pr/nC_{17}	Ph/nC_{18}	Pr/Ph	G/$C_{30}H$	C_{29}–20S	C_{29}-αββ	Ts/Ts + Tm	C_{29} Dia/reg	Hopane/sterane	C_{27}(%)	C_{28}(%)	C_{29}(%)
M11	3771.8	K_1b_1	0.44	469	0.08	18.37	0.47	0.92	0.12	0.26	0.47	0.38	0.53	0.28	1.64	42.39	22.67	34.94
LP1	3342.75	K_1b_1	0.80	453	0.60	75.38	0.36	0.47	0.53	1.43	0.26	0.55	0.64	0.79	1.06	30.71	30.73	38.56
LP1	3350.36	K_1b_1	0.98	453	0.90	90.73	0.10	0.12	0.64	0.38	0.45	0.43	0.52	0.31	1.49	33.61	23.10	43.29
LP1	3405.85	K_1b_1	0.96	451	1.03	72.58	0.15	0.21	0.62	0.20	0.34	0.43	0.60	0.45	1.52	44.75	18.82	36.43
LP1	3409.85	K_1b_1	1.25	456	1.19	83.53	0.11	0.14	0.66	0.22	0.34	0.45	0.50	0.38	1.18	44.06	19.60	36.34
Y12	3181.4	K_1b_1	0.48	443	0.36	74.81	0.41	0.33	0.79	0.30	0.48	0.43	0.49	0.28	1.62	37.80	22.69	39.50
L1	3360.5	K_1b_1	1.41	453	1.82	103.25	0.14	0.19	0.71	0.30	0.37	0.45	0.64	0.32	0.87	41.87	17.93	40.20
Y19	2332.2	K_1b_2	0.57	436	1.06	183.69	1.91	1.37	0.79	0.30	0.34	0.31	0.46	0.14	2.03	47.36	19.30	33.34
Y2	4012.66	K_1b_2	1.24	496	0.23	18.58	0.20	0.33	0.14	0.24	0.43	0.37	0.45	0.12	2.00	31.89	24.09	44.02
X11	2987.6	K_1b_2	0.48	459	0.03	6.24	0.38	0.86	0.09	0.20	0.47	0.40	0.52	0.26	2.31	36.25	22.73	41.01
Y12	2612.7	K_1b_2	3.68	436	16.34	434.98	0.27	0.78	0.33	0.70	0.51	0.49	0.37	0.09	1.55	20.13	22.61	57.26
Y12	2823.4	K_1b_2	0.49	428	0.73	147.87	0.41	0.61	0.13	0.51	0.49	0.45	0.41	0.15	1.63	28.81	23.57	47.62
L1	3180.8	K_1b_2	0.93	447	1.48	152.84	0.38	0.54	0.57	0.80	0.48	0.51	0.86	0.28	0.28	27.81	24.16	48.04
X2	2908.6	K_1b_2	0.84	442	2.11	180.13	1.76	1.81	0.87	0.82	0.56	0.59	0.72	0.61	0.22	33.66	30.98	35.36
X2	3194.6	K_1b_2	0.84	454	0.44	48.65	0.81	0.95	0.30	0.30	0.50	0.43	0.49	0.25	2.10	30.21	25.11	44.68
X6-1	2289.1	K_1b_2	1.35	436	5.81	411.28	2.73	4.84	0.47	1.51	0.40	0.41	0.35	0.17	0.36	24.71	30.06	45.23
X6-1	2327.9	K_1b_2	1.32	438	4.81	364.12	1.54	2.59	0.59	0.40	0.41	0.44	0.50	0.25	0.51	32.92	20.77	46.30
X6-1	2357.6	K_1b_2	1.48	439	6.12	413.51	0.98	1.32	0.60	0.60	0.40	0.40	0.56	0.53	1.82	50.87	16.15	32.97
X6-1	2382.3	K_1b_2	0.50	441	0.16	31.82	0.67	1.39	0.28	0.57	0.42	0.41	0.27	0.22	0.91	29.81	27.61	42.58
Y1	3055.3	K_1b_2	0.63	449	0.51	71.18	1.34	1.87	0.61	0.37	0.52	0.50	0.42	0.11	0.53	27.59	25.18	47.23
Y5	3417.8	K_1b_2	0.41	442	0.27	65.19	0.56	0.44	1.19	0.35	0.51	0.48	0.45	0.11	0.99	26.48	25.41	48.11
Y10	2393	K_1b_2	1.93	434	9.85	503.11	0.36	1.75	0.22	0.66	0.28	0.27	0.32	0.14	0.74	21.32	33.29	45.38
Y10	2412	K_1b_2	1.43	442	3.07	161.29	0.19	0.25	0.72	0.73	0.44	0.43	0.39	0.18	1.43	26.02	27.58	46.40
Y4	1689.57	K_1b_2	1.86	434	8.65	452.79	1.19	3.37	0.32	0.36	0.12	0.26	0.40	0.06	4.53	20.43	20.70	58.87
Y4	1707.4	K_1b_2	1.24	432	14.96	521.32	0.68	2.02	0.27	0.80	0.14	0.24	0.39	0.05	1.09	19.79	28.60	51.62
Y7	2181.5	K_1b_2	0.96	436	0.88	91.25	0.48	0.73	0.24	0.49	0.17	0.26	0.29	0.07	1.28	23.24	21.52	55.23
Y8	2225.6	K_1b_2	1.23	439	3.97	321.72	0.45	0.44	0.87	0.10	0.33	0.30	0.52	0.17	2.21	30.44	12.78	56.78
Y14	3609.95	K_1b_2	0.46	438	0.22	47.86	0.48	0.81	0.20	0.32	0.24	0.30	0.44	0.09	1.51	24.75	22.25	53.00
Y11	2364.52	K_1b_2	0.43	437	0.35	81.78	0.36	0.77	0.14	0.44	0.35	0.36	0.41	0.15	1.56	30.85	23.99	45.17
Y11	2675.06	K_1b_2	0.65	443	1.26	185.33	1.63	2.25	0.73	0.20	0.53	0.53	0.43	0.13	0.22	27.11	33.24	39.65
Y11	2798.74	K_1b_2	2.01	442	9.30	451.47	0.34	0.57	0.44	0.52	0.52	0.53	0.25	0.14	0.35	25.15	29.67	45.19
Y9	2414.03	K_1b_2	1.12	439	3.75	325.00	0.65	2.43	0.26	0.50	0.32	0.25	0.15	0.04	0.72	16.96	27.56	55.48
Y9	2423.43	K_1b_2	1.76	439	8.45	475.24	0.86	2.48	0.32	0.54	0.34	0.25	0.30	0.05	2.57	17.09	24.94	57.97
Y6	1771.66	K_1s_1	3.89	430	16.17	403.19	0.48	1.11	0.40	0.36	0.33	0.32	0.27	0.09	2.21	26.70	29.83	43.47
X5	1930.42	K_1s_1	0.54	442	0.30	55.78	0.50	0.93	0.10	0.27	0.47	0.38	0.36	0.23	1.44	40.35	23.51	36.14
Y2	2697.7	K_1s_1	0.56	434	0.63	101.19	1.83	4.58	0.44	0.20	0.53	0.42	0.34	0.09	0.29	29.07	26.96	43.96
Y2	2723.08	K_1s_1	0.51	438	0.32	62.63	0.54	0.42	0.98	0.05	0.49	0.40	0.29	0.22	1.54	27.98	17.14	54.88
Y2	3086.96	K_1s_1	0.40	457	0.20	49.89	0.31	0.32	0.78	0.22	0.39	0.36	0.49	0.17	2.04	33.35	22.38	44.28
L1	2429.3	K_1s_1	0.74	443	2.08	276.12	0.68	2.31	0.26	0.22	0.45	0.32	0.28	0.07	0.17	20.44	28.93	50.63
Y1	2840.55	K_1s_1	2.06	439	13.62	369.62	1.64	1.10	1.34	0.76	0.51	0.49	0.03	0.10	0.17	24.99	26.15	48.86

Note: Pr/Ph = Pristane/phytane; G/$C_{30}H$ = gammacerane/C_{30} hopanes; C_{29}–20S = C_{29} 20S/(20S + 20R) sterane; C_{29}-αββ = C_{29} αββ/(ααα+ αββ); Ts/Ts + Tm = Ts (C_{27} 18α(H) 22-29-30-trisnorneohopane)/(Ts (C_{27} 18α(H) 22-29-30-trisnorneohopane + Tm (C_{27} 17α(H)-22, 29, 30-trisnorneohopane); C_{29}Dia/reg = C_{29} diasteranes/C_{29} steranes; C_{27}(%), C_{28}(%) and C_{29}(%) represent the relative content of C_{27}–C_{29} regular steranes.
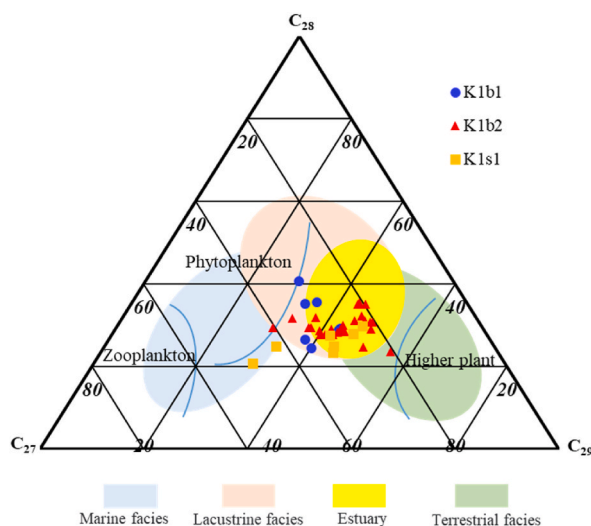
Fig. 8. Ternary diagram of regular steranes (C_{27}, C_{28}, and C_{29}) showing the organic matter inputs in the Chagan sag, Yin'e Basin.
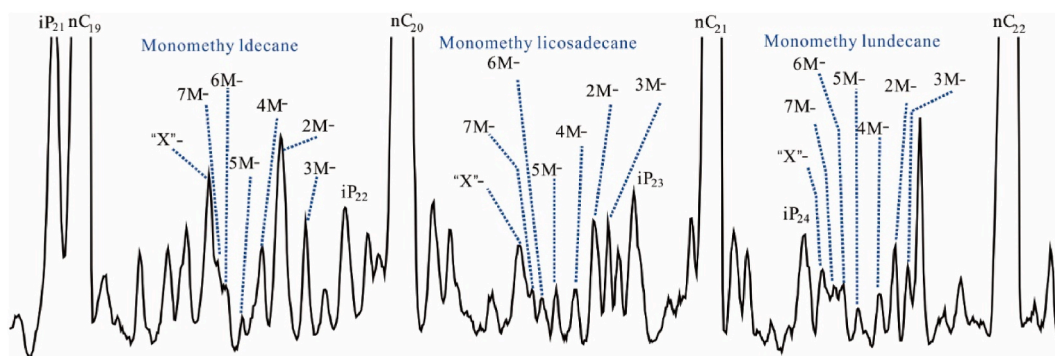

Fig. 9. Monomethyl alkanes detected by GC-MS in total ion mass spectrogram in K_1b_2 source rock.
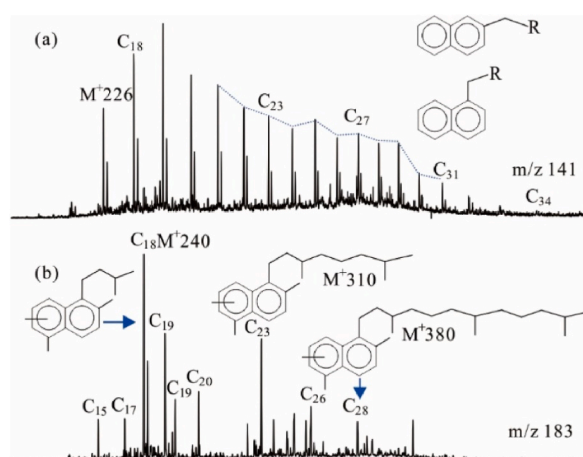

Fig. 10. The distribution of long-chain naphthalene compounds in *m/z* 141 and *m/z* 183 mass chromatogram.

heterotrophic microorganisms, which are rich in hydrogen [37,38]. The relationship of TOC and hydrogen index (HI) also reflects the influence of microbial action on the properties of organic matter in source rock from another aspect. Microorganisms also decompose and consume the original organic matter, which reduces the abundance and the hydrogen-rich degree of the original organic matter. In
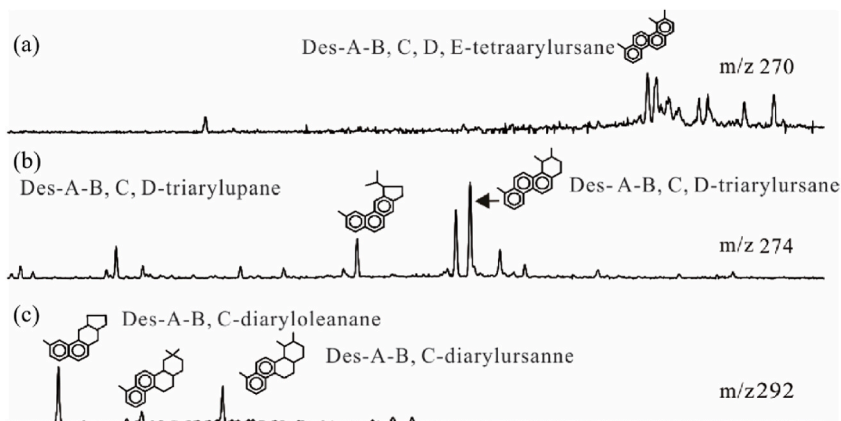
Fig. 11. Mass chromatogram of ring-A degraded triterpanes in source rock of Chagan Sag.
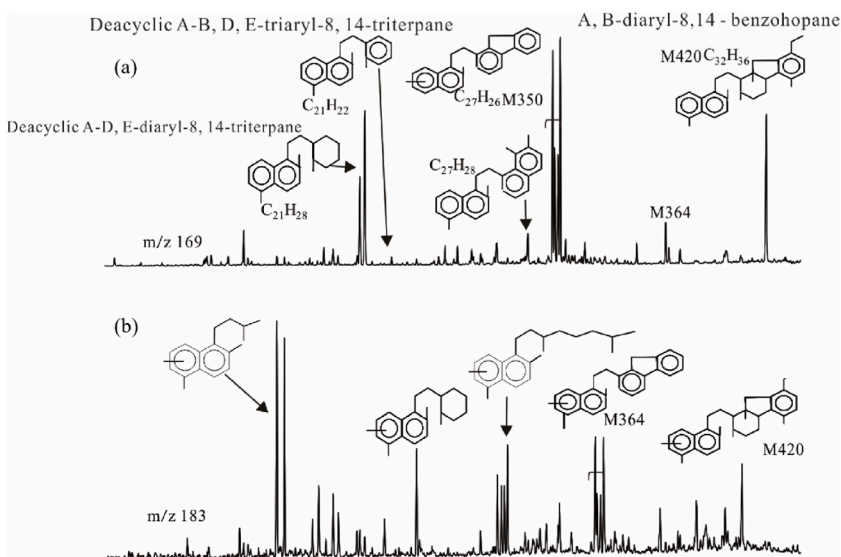
Fig. 12. Mass chromatogram of aromatic 8,14-secotriterpenes in source rock of Chagan Sag.
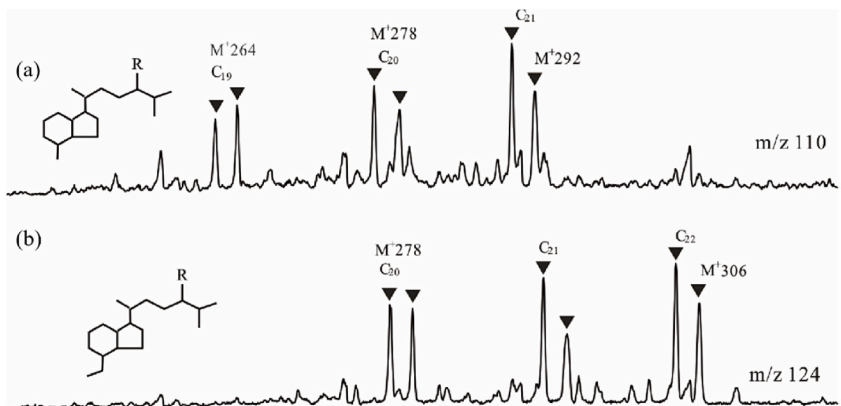

Fig. 13. Mass chromatograms of des-A, B-cyclostanes in source rock in Chagan Sag.
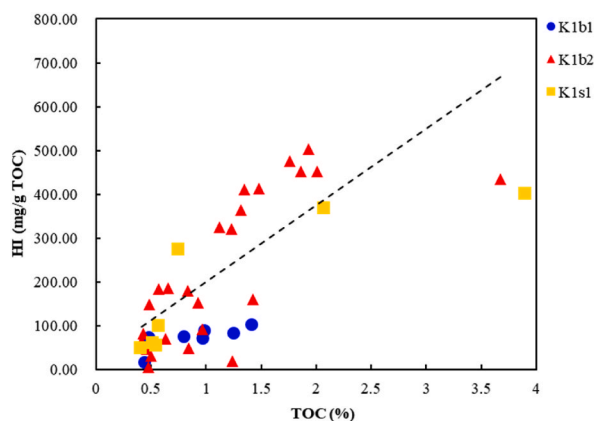
Fig. 14. Relationship between total organic matter (TOC)abundance and hydrogen index (HI) of source rock in Chagan Sag.

addition, the biochemical action stage has a universal significance in the formation of source rock. The strong reducibility of water during source rock formation in Chagan Sag is of great significance to the preservation of regenerated organic matter.

The high content of gammacerane in some samples provides stratified reductive environment, and the abnormal high amount of amorphous component and hopanes, special biomarkers also support the speculation. Based on the analysis of the maceral composition and biomarkers characteristics of source rock in Chagan Sag, the input characteristics of the morphological microscopic components of Chagan Sag primarily come from higher plants, which reflect the input characteristics of the original organic matter (Figs. 4 and 5 and Tables 1 and 2). High content of amorphous organic matter that is widely developed mainly suggest the contribution of regenerated organic matter. The composition and distribution characteristics of monomethyl paraffin compounds, long-side chain alkyl naph-thalene series compounds, de A-triterpenes with different aromatization degrees, aromatized 8, 14-triterpenes, and the abundant de A-B cyclosteranes fully reflect the contribution of microbial (bacterial) action to hydrocarbon generation (Figs. 9–13). High content of gammacerane, which indicates a density-stratified water column, provide favorable environment for the microbial action of hydro-carbon regeneration. Microorganism employs original organic matter as carbon and energy source and decompose organic matter at first. And then the well-developed organisms accelerate the formation of reducing the environment, which is conducive to the pres-ervation of organic matter. After deposition and burial, organic matter is continuously transformed by microorganisms and converted into substances that are more likely to generate hydrocarbons, such as bacteria-degraded amorphous bodies, sapropel-type kerogen [38–40]. The large number of compounds derived from bacteria or related to bacterial activities prove that microbial action has an important influence on the hydrocarbon-generating organic matter of source rock in Chagan Sag. Therefore, apart from the higher plant input, the bacterial organism also contributed the origins of the organic matter, which also exhibit from the high content of amorphous in the maceral composition.

4.3. Depositional environment

Biomarkers in the source rocks are often analyzed as indicators of organic matter source, depositional environment, and thermal maturity [24,28,29]. The distribution characteristics of pristane and phytane can reflect the depositional environment and pH value of the medium [24,26,41]. When Pr/Ph < 1, it indicates a strongly decreasing environment and when Pr/Ph > 2, and the reducibility of the sedimentary environment is relatively weak. The Pr/Ph of coal often measures greater than 2.5, and the maximum is more than 8
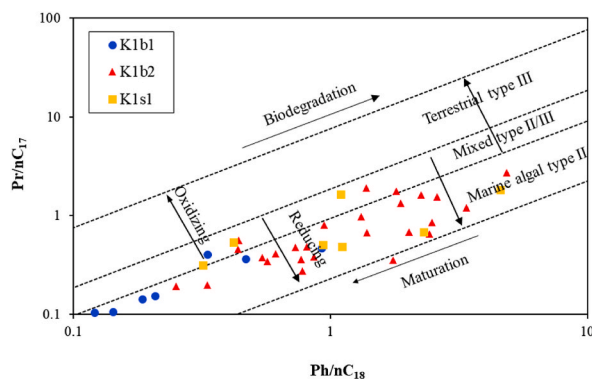

Fig. 15. Ph/nC$_{18}$ vs Pr/nC$_{17}$ ratios of source rocks in Chagan Sag.

[24]. The Pr/Ph values of soluble organic matter in the source rock of the Chagan Sag are distributed between 0.09 and 1.34, and the average values are all smaller than 0.5 (Table 3), reflecting a strong reducing depositional environment during the original organic matter sediment stage. The distribution relationship of Pr/nC_{17} and Ph/nC_{18} is commonly used to classify the source of organic matter and the type of depositional environment [28,42]. Maturation biodegradation are the major factors responsible for the differences in crude oil composition. Ratios less than 1.0 are indicative of non-biodegraded oils [29]. The Pr/nC_{17} and Ph/nC_{18} values of source rock in Chagan Sag are distributed between 0.10–2.73 and 0.12–4.84 (Fig. 15, Table 3), which are mainly algae type II and mixed Type II/III from strongly reduced environment. In addition, the ratio is also affected by maturity [43]. Fig. 15 shows that the level of maturity of the K_1b_1 source rock is much higher than K_1b_2 and K_1s_1, and biodegradation was not observed (Fig. 15).

Gammaceranes are primarily developed in strongly reducing and high-salt environments [25]. The gammacerane index is the ratio of gammacerane to C_{30} hopane that can reflect the differences in sedimentary environments [25,42]. Gammaceranes are widely distributed in saturated hydrocarbons in the source rock of Chagan Sag with the index of gammacerane ranges from 0.05 to 1.51, with an average of 0.46 (Fig. 16, Table 3). The gammacerane index of K_1b_1 ranges from 0.2 to 1.43, with an average value of 0.44 (Table 3). The gammacerane index of K_1b_2 and K_1s_1 ranges from 0.1–1.51 and 0.05–0.76, respectively (Fig. 16, Table 3). The overall characteristics of the gammacerane index (Gammacerane/C_{30} hopane) distribution are basically correlated with the environmental significance of Pr/Ph (Fig. 16, Table 3). The ratios of Pr/Ph and Gammacerane index show most samples are from reduced environment and the reductive degree for K_1b_2 is much stronger (Fig. 16).

4.4. Thermal maturity

The thermal alteration of organic matter in the analyzed samples is also demonstrated by C_{29} 20S/(20S + 20R) and C_{29} ββ/(ββ + αα) ratios of C_{29} steranes [44]. The ratios of C_{29} 20S/(20S + 20R) and ββ/(ββ + αα) are greater than 0.35 and 0.40, respectively, suggesting these source rocks reached the oil window [24]. In this study, the C_{29} 20S/(20S + 20R) and ββ/(ββ + αα) sterane ratios for extracted source rock samples are found to be in the range of 0.12–0.56 and 0.24–0.59, respectively (Table 3). Most of analyzed samples are in the mature stage, and several samples are shown in the low-mature stage (Fig. 17a, Table 3). Samples from K_1b_1 and K_1s_1 reach the mature stage, while for K_1b_2, the maturity range is quite wide, which is consistent with rock-eval results (Figs. 17a and 3). Ts (C_{27} 18α (H) 22-29-30-trisnorneohopane) and Tm (C_{27} 17α(H)-22, 29, 30-trisnorneohopane) are important compound used for thermal maturity assessment and the ratio Ts/(Ts + Tm) is also maturity dependent. Ts (C_{27} 18α(H) 22-29-30-trisnorneohopane) and Tm (C_{27} 17α(H)-22, 29, 30-trisnorneohopane) are important compound used for thermal maturity assessment and the ratio Ts/(Ts + Tm) is also maturity dependent. Ts is more stable to thermal maturity than Tm. C_{29} diasteranes/steranes ratios also influenced by maturity. With maturity increase, the diasteranes is more stable than the regular steranes [44]. The Ts/(Ts + Tm) ratio of the analyzed samples ranges from 0.03 to 0.86 with an average of 0.43. C_{29} diasteranes/steranes ratios of the analyzed samples range from 0.04 to 0.79 with an average of 0.21 (Fig. 17 b, Table 3), showing samples from K_1b_1 are more mature than others (Fig. 17b). The results are generally consistent with the C_{29} regular sterane ratios (Fig. 17).

5. Conclusions

(1) The total organic matter of the analyzed samples ranges from 0.4 wt% ~3.89 wt% with an average of 1.12 wt%, indicating fair to excellent hydrocarbon generation potential. The rock-eval results show that the S_1+S_2 and hydrocarbon index range from 0.03–16.34 (avg.3.6) and 6.24–521.32 mg/g (avg. 199.63 mg/g), suggesting most of the kerogen types are type II and III, with small amount of type I. The Tmax ranges from 428 to 496 °C, suggesting low mature to mature stage.
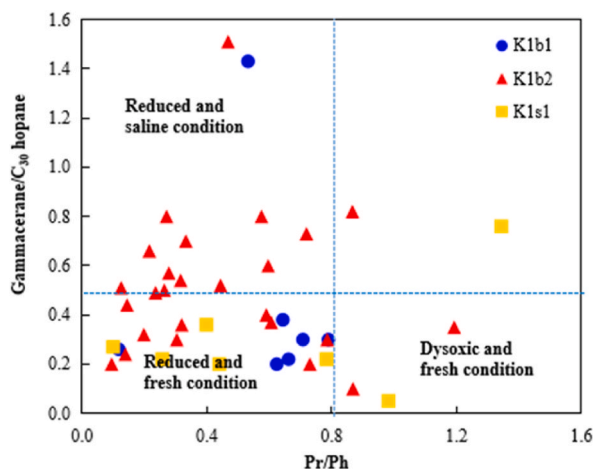

Fig. 16. Plot of Gammacerane/C_{30} hopane vs. Pr/Ph showing the depositional environment of the source rocks.
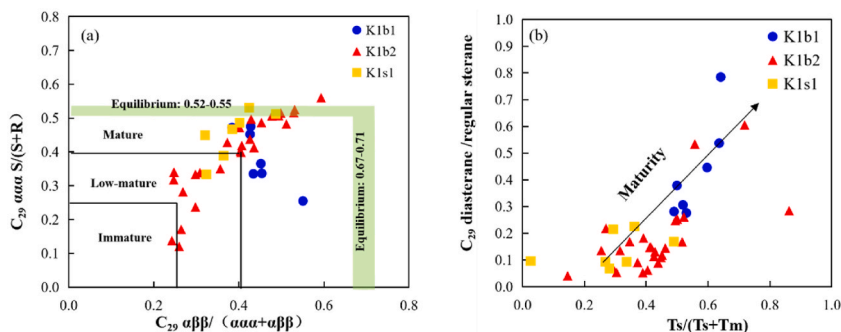
Fig. 17. C_{29} sterane 20S/(20S + 20R) vs. (αα+ββ) (a) and Ts/(Ts + Tm) vs. C_{29} diasterane/regular sterane (b) showing the thermal maturity of analyzed source rocks in Chagan Sag.

(2) The macerals component of morphological macerals presents with certain amount of vitrinite, liptinite and some inertinite. However, the amorphous component takes the dominant part of the macerals with account of 50%–80%. The amorphous components are dominated by sapropelite in the source rock, indicating bacteriolytic amorphous promote the organic generation process.

(3) Hopanes and sterane are widely distributed in the source rocks. The biomarker results show a mix of planktonic-bacterial and higher plant origins with wide range of thermal maturity and relatively reducing depositional environment. Abnormal high content of hopanes were observed in the biomarkers, and some special biomarkers such as monomethylalkanes, long-chain-alkyl naphthalenes, aromatized de A-triterpenes, 8,14-seco-triterpenes, and A, B-cyclostane are detected in Chagan Sag. The presence of these compounds suggests that bacterial and microorganisms are of great significance to the generation of hydrocarbon in the source rock in Chagan Sag.

Author contribution statement

Wenjie Xiao: Performed the experiments; Analyzed and interpreted the data; Wrote the paper.
Hong Ji: Conceived and designed the experiments; Analyzed and interpreted the data; Wrote the paper.
Guanghui Huang: Conceived and designed the experiments; Contributed reagents, materials, analysis tools and data.

Funding statements

Data availability statement

Data included in article.

Declaration of interest's statement

The authors declare no conflict of interest.

Acknowledgments

References

[1] Y.Y. Zhou, Z. Ji, B.J. Shen, Y.F. Yang, N.S. Qiu, Tenger, Research progress on main controlling factor of hydrocarbon–forming organisms in gas–bearing property, Bull. China Soc. Mineral Petrol. Geochem. 36 (2017) 332–338.
[2] Y.Y. Zhang, Z.L. He, S.F. Lu, S. Jiang, D.S. Xiao, S.X. Long, B. Gao, W. Du, J.H. Zhao, G.H. Chen, Y.C. Li, Characteristics of microorganisms and origin of organic matter in wufeng formation and Longmaxi formation in Sichuan basin, south China, Mar. Petrol. Geol. 111 (2020) 363–374.
[3] C.R. Love, E.C. Arrington, K.M. Gosselin, Microbial production and consumption of hydrocarbons in the global ocean, Nat. Microbiol. 6 (2021) 489–498.
[4] B.J. Katz, Controlling factors on source rock development: a Review of productivity, preservation, and sedimentation rate, in: N.B. Harris (Ed.), The Deposition of Organic–Carbon–Rich Sediments: Models, Mechanisms, and Consequences, vol. 82, Special Publication–Society for Sedimentary Geology, 2005, pp. 7–16.
[5] Y. Li, T. Zhang, G. Ellis, D.Y. Shao, Depositional environment and organic matter accumulation of upper Ordovician–lower Silurian marine shale in the upper Yangtze platform, south China, Palaeogeogr, Palaeoclimatol., Palaeoecol. 466 (2017) 252–264.
[6] A.N. Ding, The formation of type–D bacteride compamorphinite and its hydrocarbon generating pattern, Acta Geol. Sin. 32 (1997) 221–228.

[7] A.C. Cook, N.R. Sherwood, Classification of oil shales, coals and other organic–rich rocks, Org. Geochem. 17 (1991) 211–222.
[8] M. Ercegovac, A. Kostic, Organic facies and palynofacies: nomenclature, classification and applicability for petroleum source rock evaluation, Int. J. Coal Geol. 68 (2006) 70–78.
[9] Y.H. Zuo, C.C. Wang, S.L. Tang, Q.Q. Hao, Mesozoic and Cenozoic thermal history and source rock thermal evolution history in the Chagan Sag, Inner Mongolia, Earth Sci. J. China Univ. Geosci. 38 (2013) 553–560.
[10] W.D. Lin, Geochemical characteristics of crude oil and correlation of source rock in Chagan sag, Oil Gas Geol. 21 (2000) 249–252.
[11] J.P. Chen, Z.H. He, D. Wei, J. Qin, J. Guo, Geochemical characteristics of oil and source rock correlation in the Chagan sag of Yingen–e'jinaqi basin, NW China, Acta Sedimentol. Sin. 19 (2001) 298–305.
[12] X. Wang, Y. Wang, S. Liu, F.Q. Yang, L. Shi, Hydrocarbon accumulation pattern and exploration direction in Baiyinchagan sag of Erlian basin, Pet. Geol. Exp. 34 (2012) 291, 290.
[13] Y.H. Zuo, W. Zhang, Z.Y. Li, Z.L. Lin, Q.Q. Hao, J. Hu, Mesozoic and Cenozoic tectono–thermal evolution history in the Chagan sag, Inner Mongolia, Chin. J. Geophys. 58 (2015) 325–339.
[14] Z. Niu, Liu G, C. Zhe, Peng W, J. Chang, K. Zhang, Reservoir characteristics and hydrocarbon accumulation in Chagan Sag,Yingen–e'jinaqi Basin, Pet. Geol. Exp. 1 (2016) 36–43+111.
[15] National Bureau of Petroleum and Chemical Industry. Maceral Analysis on Polished Surfaces of Whole Rocks, SY/T, 2004, p. 6414.
[16] K.E. Peters, M.R. Cassa, Applied source-rock geochemistry, in: L.B. Magoon, W.G. Dow (Eds.), The Petroleum System. From Source to Trap, Am. Assoc. Pet. Geol. Bull., Tulsa, 1994, pp. 93–120.
[17] J.W. Deming, J.A. Baross, The early diagenesis of organic matter: bacterial activity, in: M.H. Engel, S.A. Macko (Eds.), Org. Geochem. Topics in Geobiology, vol. 11, Springer, Boston, MA, 1993.
[18] H.R. Harvey, S.A. Macko, Catalysts or contributors? Tracking bacterial mediation of early diagenesis in the marine water column, Org. Geochem. 26 (1997) 531–544.
[19] Q.Y. Wu, Y.T. Song, G.Y. Sheng, Study of molecular Organic Geochemistry on hydrocarbons originated from micro–organisms, Bulletin Nat. Sci. Found. China 2 (1997) 97–103.
[20] P.A. Meyers, R. Ishiwatari, The early diagenesis of organic matter in lacustrine sediments, in: M.H. Engel, S.A. Macko (Eds.), Organic Geochemistry Topics in Geobiology, vol. 11, Springer, Boston, MA, 1993.
[21] M. Pacton, G.E. Gorin, C. Vasconcelos, Amorphous organic matter—experimental data on formation and the role of microbes, Rev. Palaeobot. Palynol. 166 (2011) 253–267.
[22] R.Y. Al–Obaidi, T.K. Al–Ameri, Palynofacies, palaeoenvironment, and source rocks evaluation of ratawi formation, southern Iraq, Arabian J. Geosci. 6 (2013) 3303–3312.
[23] X. Luo, Z. Zhao, Y. Meng, Application of an odd/even predominance of n–alkanes in oil–source rock correlation: taking the lower Paleozoic strata of the Tarim Basin as an example, Environ. Toxicol. Chem. 97 (2015) 409–416.
[24] K.E. Peters, C.C. Walters, J.M. Moldowan, The Biomarker Guide, vol. 2, Cambridge University Press, Cambridge, 2005.
[25] J.S. Sinninghe Damsté, F. Kenig, M.P. Koopmans, J. Koster, S. Schouten, J.M. Hayes, J.W. de Leeuw, Evidence for gammacerane as an indicator of water column stratification, Geochem. Cosmochim. Acta 59 (1995) 1895–1900.
[26] G. Ourisson, M. Rohmer, Hopanoids 2. Biohopanoids: a novel class of bacterial lipids, Acc. Chem. Res. 25 (1992) 403–408.
[27] G.Y. Sheng, L.U. Hong, J. Liao, Advances on novel hopanoids present in geological bodies, Geochimica 5 (2019) 3–28.
[28] B.P. Tissot, D.H. Welte, Petroleum Formation and Occurrence, Edition, Springer-Verlag, Berlin, 1984, pp. 643–644. Second Revised and Enlarged.
[29] B.M. Didyk, B.R.T. Simoneit, S.C. Brassell, G. Eglinton, Organic geochemical indicators of palaeoenvironmental conditions of sedimentation, Nature 272 (1978) 216–222.
[30] Y.V. Kissin, Catagenesis and composition of petroleum: origin of n–alkanes and isoalkanes in petroleum crudes, Geochem. Cosmochim. Acta 51 (1987) 2445–2457.
[31] B. Sherwood, Lollar, T.D. Westgate, J.A. Ward, G.F. Slater, G. Lacrampe-Couloume, Abiogenic formation of alkanes in the Earth's crust as a minor source for global hydrocarbon reservoirs, Nature 416 (2002) 522–524.
[32] T.G. Wang, D. Zhu, H. Lü, Z.H. Zhang, J.Q. Sun, Q.J. Liao, High molecular weight n–alkanes of high–waxy condensate and its source kitchen orientation in the Qianmiqiao burial–hill zone, Bohai Gulf Basin, Chin. Sci. 3 (2004) 255–264.
[33] Q.S. Cheng, M. Zhang, G.H. Huang, Even–carbon predominance of monomethyl branched alkanes in humic coal from Junggar Basin, NW China, Acta Geochimica (Engl. Transl.) 39 (2020) 434–444.
[34] L. Ellis, S.J. Fisher, R.K. Singh, Long–chain alkylnaphthalenes in crude oils and sediments, September, in: Presented at the 19th international Meeting on Organic Geochemistry., Istanbul, 1999, pp. 6–10.
[35] A.D. Woodhouse, J.N. Oung, R.P. Philp, Triterpanes and ring—a degraded triterpanes as biomarkers characteristic of tertiary oils derived from predominantly higher plant sources, Org. Geochem. 18 (1992) 23–31.
[36] N. Ma, D. Hou, H. Shi, Novel tetracyclic terpanes in crude oils and source rock extracts in pearl river mouth basin and their geological significance, J. Earth Sci. 25 (2014) 713–718.
[37] B. Zhang, Y.Y. He, Y. Chen, Q.Y. Meng, Geochemical characteristics and oil accumulation of significance of the high quality saline lacustrine source rocks in the western Qaidam Basin, NW China, Acta Pet. Sin. 38 (2017) 1158–1167.
[38] T.G. Wang, N. Zhong, Z.H. Yu, On bacterial role in hydrocarbon generation mechanism, in: Banqiao Sag, Science in China: Series B, 38, 1995, pp. 1123–1134.
[39] M. Kuypers, P. Blokker, E.C. Hopmans, Archaeal remains dominate marine organic matter from the early albian oceanic anoxic event 1b, Palaeogeogr. Palaeoclimatol. Palaeoecol. 185 (2002) 211–234.
[40] W.C. Wang, C. Wang, M.Z. Sun, Effect of microorganisms during diagenesis and its significance on petroleum formation, Nat. Gas Geosci. 11 (2016) 1970–1978.
[41] H.T. Haven, J. Rullkötter, J.De Leeuw, Pristane/phytane ratio as environmental indicator, Nature 333 (1988) 604.
[42] K.E. Peters, M.G. Fowler, Applications of petroleum geochemistry to exploration and reservoir management, Org. Geochem. 33 (2002) 5–36.
[43] M.A. Younes, R.P. Philp, Source Rock Characterization based on biological marker distribution of crude oils in the Southern Gulf of Suez, Egypt, J. Petrol. Geol. 28 (2005) 301–317.
[44] W. Seifert, J.M. Moldowan, Use of biological markers in petroleum exploration, Methods Geochem. Geophys. 24 (1986) 261–290.